Available online at www.sciencedirect.com
SCIENCE DIRECT®
Journal of Chromatography A, 1028 (2004) 121–137
JOURNAL OF CHROMATOGRAPHY A
www.elsevier.com/locate/chroma

Band splitting in overloaded isocratic elution chromatography III. Modeling of adsorbate–adsorbate interactions by a two-component extension of a BET kinetic isotherm model

Fabrice Gritti [a,b], Georges Guiochon [a,b,*]

[a] *Department of Chemistry, University of Tennessee, Knoxville, TN 37996-1600, USA*
[b] *Division of Chemical Sciences, Oak Ridge National Laboratory, Oak Ridge, TN 37831-6120, USA*

Received 15 July 2003; received in revised form 17 November 2003; accepted 19 November 2003

Abstract

A new two-component competitive adsorption model was derived to account for the competitive adsorption data of mixtures of ethylbenzoate and 4-*tert*-butylphenol, on a C_{18}-Kromasil column under RPLC conditions (mobile phase, methanol/water, 62/38, v/v). The derivation is based on kinetic arguments and is an extension to multicomponent systems of the single-component BET isotherm. The model assumes that the molecules of the first compound (A) can adsorb on layers made of molecules of either A or B, while molecules of B can only adsorb on layers made of molecules of A. This makes the competitive isotherm consistent with the single-component isotherms of ethylbenzoate and 4-*tert*-butylphenol, the multilayer BET and the monolayer Langmuir isotherm models, respectively. The competitive adsorption data were acquired by frontal analysis (FA) with equimolar mixtures of eight different concentrations. For the seven lowest concentrations, these data were derived from the retention times of the shocks of the two compounds and the concentration of the intermediate plateau of the less retained compound. At the highest concentration (25 g/l), the individual band profiles were measured by collecting and analyzing twenty fractions. The low concentration data ($C \leq 10$ g/l) are well accounted for by the two competitive isotherm models derived previously but these models fail to describe the experimental data of 4-*tert*-butylphenol at high concentrations. By contrast, the new model predicts very well the experimental adsorption data for mixtures of ethylbenzoate and 4-*tert*-butylphenol in the whole range of concentration studied. Our results suggest that the adsorption constant of 4-*tert*-butylphenol onto layers made of ethylbenzoate ($b_{B,A} = 0.0120$ l/g) is intermediate between those of ethylbenzoate on layers made of 4-*tert*-butylphenol ($b_{A,B} = 0.0105$ l/g) and of ethylbenzoate on itself ($b_{A,A} = 0.0145$ l/g). This new model should give an improved description of the band splitting observed for 4-*tert*-butylphenol in the presence of ethylbenzoate.
© 2004 Elsevier B.V. All rights reserved.

Keywords: Adsorption equilibrium; Frontal analysis; Band splitting; Extended BET isotherm; Isotherm modeling; Competitive isotherm; Ethylbenzoate; 4-*tert*-Butylphenol

1. Introduction

Elution band profiles at high concentrations are essentially controlled by the thermodynamics of the phase equilibrium involved, unless the mass transfer kinetics is slow [1–3]. Accordingly, the recovery yield and the production rate that can be achieved for a given industrial separation depend largely on this thermodynamics, i.e., on the competitive equilibrium isotherms of the feed components. For obvious economic reasons, preparative chromatography must be carried out at high concentrations. Under such conditions, the equilibrium isotherms of the feed components between the two phases of the chromatographic system are rarely linear. The stronger the non-linear behavior of the isotherm at the maximum concentration of the band, the more skewed the band profile and the lower the resolution of the band from its neighbors, hence the lower the recovery yield and/or the production rate for a given purity [1]. This non-linear behavior affects the resolution between bands at all column efficiencies, particularly because it causes intense competition for adsorption between the components that are not or are poorly resolved [1]. To a lesser degree, the mass transfer kinetics affects the precise shape of the elution bands, adding to the profiles predicted by thermodynamics alone a certain amount of axial

* Corresponding author. Tel.: +1-865-974-0733; fax: +1-865-974-2667.
E-mail address: guiochon@utk.edu (G. Guiochon).

0021-9673/$ – see front matter © 2004 Elsevier B.V. All rights reserved.
doi:10.1016/j.chroma.2003.11.088

dispersion and smoothing their edges. For these reasons, the use of computer-assisted optimization in the development of new applications of preparative liquid chromatography requires the prior determination of accurate thermodynamic and kinetic data and the proper modeling of these data, i.e., the derivation of the competitive isotherms of the feed components and of the rate coefficients of the various steps involved in the mass transfer kinetics across the column [1–4].

Numerous methods are available for the acquisition of equilibrium isotherm data and for the derivation of single-component isotherms [1,5]. Frontal analysis (FA) [1,5–7], elution by characteristic point (ECP) [1,8,9], and the pulse method [1,10] are the most accurate, the fastest, and the most convenient, respectively. These methods have other advantages and drawbacks which must be taken into account in any specific case, in order to minimize the errors of measurement and their costs [1]. By contrast, investigations of binary or competitive equilibria remain far more difficult [11–17]. The acquisition of competitive isotherm data by FA or by the pulse method is a far more ambitious project than that of the measurement of single-component isotherms. So, the preferred method of derivation of competitive isotherms consists in deriving them from the single-component isotherms of the components of the mixture involved [1,5,11,14,17]. For this purpose, assumptions must be made as to whether the adsorbed and the bulk liquid phases are ideal or not.

In the specific case of ethylbenzoate and 4-*tert*-butylphenol, we previously derived a new competitive adsorption isotherm on the basis of kinetic arguments [18], assuming that molecules of one of two components may adsorb on those of the second one already adsorbed but that the converse was forbidden. The corresponding single-component isotherms, i.e., the isotherms obtained for one component when the concentration of the other one is zero were the extended liquid–solid BET and the Langmuir isotherms. Conversely, using these two single-component isotherms, we could derive, using the IAS theory, a thermodynamically-consistent competitive binary isotherm model corresponding to these two single-component isotherms [18]. These two sets of competitive isotherm models were compared with respect to the accuracy of their predictions of the experimental band profiles of large samples of binary mixtures of ethylbenzoate and 4-*tert*-butylphenol (40 g/l each), using a packed Kromasil-C_{18} column and a mixture of methanol and water (62/38, v/v) as the stationary and mobile phase, respectively [18,19]. Unexpected splitting of the band profile of 4-*tert*-butylphenol was observed under these experimental conditions. Both sets of competitive isotherms predicted the peak splitting of 4-*tert*-butylphenol but did not account quantitatively for the phenomenon. Calculations of the band profiles using the equilibrium-dispersive model of chromatography predicted that the second band of 4-*tert*-butylphenol accounted for only less than 0.2% of the total amount injected, instead of 5% measured. The hypothesis of an ideal mixture in the adsorbed phase was certainly erroneous. Also, the fact that 4-*tert*-butylphenol could not be covered by any higher layer of molecules of ethylbenzoate might be too strong a constraint in the model and should be released. As suggested by one reviewer of our previous work, some competitive adsorption data should be acquired to test these competitive adsorption models.

In this work, we acquired the adsorption data of equimolar mixtures of ethylbenzoate and 4-*tert*-butylphenol at eight concentrations, on the same C_{18}-Kromasil column and with the same methanol/water (62/38, v/v) mobile phase as in the previous work, using frontal analysis extended to binary mixtures. The competitive binary isotherm models derived earlier did not account well for these experimental data. So, we extended these models by releasing the main constraint and allowing the adsorption of molecules of ethylbenzoate on layers made of molecules of 4-*tert*-butylphenol molecules. Assumptions regarding the equilibrium between neighboring layers and layers that are not directly in contact with the mobile phase are necessary to derive the composition of the adsorbed phase. This severely complicates the calculations of the multicomponent adsorption isotherms and leads to an isotherm that can be determined only numerically. The experimental adsorption data and the prediction of the new model are compared.

2. Theory

2.1. Determination of two-component isotherms by competitive frontal analysis

Among the various chromatographic methods available to determine the competitive isotherms of two components, frontal analysis (FA) is the most accurate [1,20]. When the two compounds, 1 and 2, exhibit two front shocks and when the front shock of compound 1 appears first, a simple integral mass balance of the binary mixture gives:

$$q_1^* = \frac{(V_1 - V_0)C_1^* - (V_2 - V_1)(C_1^i - C_1^*)}{V_{\text{ads}}} \quad (1)$$

$$q_2^* = \frac{(V_2 - V_0)C_2^*}{V_{\text{ads}}} \quad (2)$$

where q_1^* and q_2^* are the equilibrium concentrations of the two components in the adsorbed phase; V_0, V_1, V_2 and V_{ads} are the column dead volume, the elution volumes of the two breakthrough fronts, and the volume of adsorbent in the column, respectively; C_1^*, C_2^* and C_1^i are the feed concentrations of components 1 and 2 and the concentration of component 1 in the intermediate plateau, respectively. Accordingly, the single-component calibration curve of component 1 is necessary to measure C_1^i at the column outlet.

Compared to the use of FA for the determination of single-component isotherms, the determination of the calibration curve of the detector is the only additional difficulty encountered in the use of FA for the determination of

binary isotherms. It must be emphasized, however, that the method is accurate only insofar as there is an intermediate plateau of component 1, i.e., that the breakthrough front of the binary mixture has an horizontal inflection tangent that separate two steep shock layers.

2.2. Models of single-component isotherm

The problem consists in finding a suitable isotherm model to account for the competitive adsorption behavior of two compounds, ethylbenzoate and 4-*tert*-butylphenol, knowing their single-component isotherms. The problem is complex because these two isotherms are quite different and the elution profiles of binary mixtures are unusual, exhibiting the consequences of a reversal of the elution order at high concentrations.

2.2.1. The Langmuir isotherm

This model, which is the most frequently used in studies of liquid–solid chromatographic equilibria, describes well the adsorption behavior of pure 4-*tert*-butylphenol on the C_{18}-Kromasil column used in this work [18]. It is written:

$$q^* = \frac{q_s b C}{1 + bC} \tag{3}$$

In this model, q_s is the monolayer saturation capacity of the adsorbent and b is the equilibrium constant of adsorption. This model assumes that the surface of the adsorbent is homogeneous, that the adsorption is localized, and that there are no adsorbate–adsorbate interactions.

2.2.2. The extended liquid–solid multilayer BET model

The adsorption behavior of ethylbenzoate on the C_{18}-Kromasil column used here is well accounted for by an extension of the BET model initially derived by Brunauer, Emmett, and Teller [18]. It is the most widely applied isotherm model in studies of gas-solid equilibria. This model assumes multilayer adsorption and was developed to describe adsorption phenomena in which successive molecular layers of adsorbate form at pressures well below the pressure required for the completion of the monolayer [5]. The formulation of the extension of this model to liquid–solid chromatography was derived and detailed earlier [21]. Its final equation is:

$$q^* = q_s \frac{b_S C}{(1 - b_L C)(1 - b_L C + b_S C)} \tag{4}$$

where q_s is the monolayer saturation capacity of the adsorbent, b_S is the equilibrium constant for surface adsorption–desorption over the free surface of the adsorbent and b_L is the equilibrium constant for surface adsorption–desorption over a layer of adsorbate molecules. This model accounts for local adsorption.

A variant of this isotherm model, which is more realistic in liquid–solid adsorption, assumes that only a finite number, N, of adsorbate layers is formed. The equation of this new model is [22]:

$$q^* = q_s \frac{1 - (N+1)(b_L C)^N + N(b_L C)^{N+1}}{(1 - b_L C)^2 (1/b_S C + (1 - (b_L C)^N / 1 - b_L C))} \tag{5}$$

This last model will be the single-component isotherm consistent with the competitive model that is derived in a later section.

2.3. Models of binary competitive adsorption isotherm

In a precedent paper [18], we derived two models of competitive adsorption isotherms in an attempt to describe the individual elution band profiles of the two compounds in mixtures of 4-*tert*-butylphenol and ethylbenzoate. We summarize their equations.

2.3.1. Binary Langmuir–BET competitive isotherm derived from the IAS theory

Using the framework of the IAS theory extended to liquid–solid equilibria [23,24], the following competitive isotherm equations were derived [18]:

$$\frac{q_A}{q_S} = \frac{[b_{A,S} + b_{A,A} b_{B,S} C_B] C_A}{(1 - b_{A,A} C_A)(1 - b_{A,A} C_A + b_{A,S} C_A + b_{B,S} C_B)}$$
$$\frac{q_B}{q_S} = \frac{[b_{B,S} - b_{A,A} b_{B,S} C_A] C_B}{(1 - b_{A,A} C_A)(1 - b_{A,A} C_A + b_{A,S} C_A + b_{B,S} C_B)} \tag{6}$$

where A and B stand for the single components whose adsorption isotherms are described by the BET and the Langmuir isotherm models, respectively. $b_{A,S}$ and $b_{B,S}$ are the adsorption constants of the molecules of A and B on the adsorbent surface, respectively. $b_{A,A}$ is the adsorption constant of molecules of A on a layer made of molecules of A. The model assumes an ideal behavior for the mixture of ethylbenzoate and 4-*tert*-butylphenol in the adsorbed phase and that the saturation capacity q_S is the same for the two compounds. Using the framework of the IAS theory, no interaction parameter is introduced between the two compounds and all the parameters of the binary competitive isotherm are those of the two single-component isotherms.

2.3.2. Binary Langmuir–BET competitive isotherm derived from kinetic arguments

The following five assumptions are made regarding the adsorption behavior of the two compounds A and B:

(I) The adsorption and desorption of A and B follow a first order kinetics.
(II) Molecules of both A and B may adsorb on either the solid surface or on adsorbed molecules of A.
(III) Molecules of neither A nor B may adsorb on adsorbed molecules of B.
(IV) The adsorbed phase is composed of a finite number N of layers.

(V) The total monolayer capacity for A and B are not the same ($q_{s,A} \neq q_{s,B}$). Both are independent of the number of the layers in the multilayer system.

These assumptions result in the following binary competitive adsorption model when N tends towards infinite [18]:

$$\frac{q_A}{q_{s,A}} = \frac{b_{A,S}C_A + b_{A,S}b_{B,A}C_AC_B}{(1 - b_{A,A}C_A)[1 - b_{A,A}C_A + b_{A,S}C_A + b_{B,S}C_B + (b_{A,S}b_{B,A} - b_{B,S}b_{A,A})C_AC_B]} \quad (7)$$

$$\frac{q_B}{q_{s,B}} = \frac{b_{B,S}C_B + (b_{A,S}b_{B,A} - b_{B,S}b_{A,A})C_AC_B}{1 - b_{A,A}C_A + b_{A,S}C_A + b_{B,S}C_B + (b_{A,S}b_{B,A} - b_{B,S}b_{A,A})C_AC_B} \quad (8)$$

where $b_{B,A}$ is the adsorption constant of the B molecules on layers made of A molecules. This is a new, independent parameter that is introduced in the kinetic competitive model, in addition to the parameters of the single-component isotherms. It accounts for the interactions between molecules of B and the molecules of A on which they are adsorbed. It does not exist in the IAS model derived above.

2.4. Extension of the kinetic binary competitive adsorption isotherm

The precedent kinetic model was extended by allowing the adsorption of molecules of A on molecules of B. This introduces another intermolecular interaction parameter.

2.4.1. Assumptions of the second kinetic model

I The adsorption and desorption of A and B follow a first order kinetics.
II Molecules of both A and B may adsorb on either the solid surface or on adsorbed molecules of A.
III Molecules of A may adsorb on adsorbed molecules of B. Molecules of B cannot adsorb on other molecules of B already adsorbed. This is the implementation to the precedent model.
IV The adsorbed phase is composed of a finite number, N, of layers, as shown in Fig. 1.
V The total monolayer capacity for A and B are not necessarily the same ($q_{s,A} \neq q_{s,B}$). Both are independent of the number of the layer in the multilayer system.

Assumption III is the new one. It would be inconsistent to assume that B molecules can adsorb on other B molecules because the single-component isotherm of B is accounted for by the Langmuir model which excludes any interactions between adsorbate molecules.

2.4.2. Definitions

The following parameters are used in the derivation of the adsorption isotherm model. Their definitions are illustrated in Fig. 1 and formulated below.

- $q_{s,A}$ and $q_{s,B}$ are the monolayer capacities of components A and B, respectively.

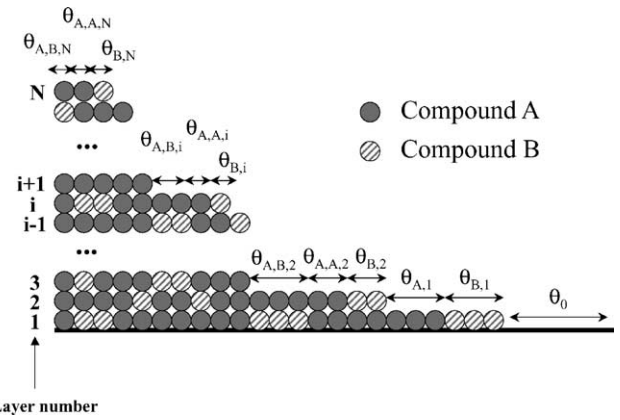

Fig. 1. Scheme of the two-component adsorption model. Note the structure of the adsorbed system due to the non-adsorption of compound B on itself.

- θ_0 is the fractional surface coverage of the adsorbent that is free from adsorbate (but for solvent molecules).
- $\theta_{A,A,i}$ is the fractional surface coverage of layer i that is occupied by molecules of A, is not covered by any higher layer of adsorbate molecules, and covers molecules of A in the layer $i-1$ (with $2 \leq i \leq N$). For $i = 1$, the fractional surface coverage of layer 1 that is occupied by A molecules on the adsorbent and not covered by any layer of adsorbate molecules is $\theta_{A,1}$.
- $\theta_{A,B,i}$ is the fractional surface coverage of layer i that is occupied by molecules of A, is not covered by any higher layer of adsorbate molecules, and covers molecules of B in the layer $i-1$ (with $2 \leq i \leq N$).
- $\theta_{A,i} = (\theta_{A,A,i} + \theta_{A,B,i})$ (with $2 \leq i \leq N$).
- $\alpha_i = \theta_{A,A,i}/\theta_{A,i}$. This parameter represents the fraction of the molecules of A that are present in the upper layer i adsorbed on molecules of A. Hence, $1 - \alpha_i = \theta_{A,B,i}/\theta_{A,i}$ represents the fraction of the molecules of A that are in the upper layer i adsorbed on molecules of B.
- $\theta_{B,i}$ is the fractional surface coverage of layer i that is occupied by B molecules and, according to the assumptions of the model, covers the layer $i-1$ of adsorbate molecule A (with $2 \leq i \leq N$). $\theta_{B,1}$ is the fractional surface coverage of the adsorbent surface by B molecules.
- $\varphi_{A,A,k,i}$ is the fraction of the surface area of layer k that is occupied by molecules of A that covers molecules of A trapped below the upper layer i ($2 \leq i \leq N$) that is not covered by any higher layer of adsorbate (with $1 \leq k \leq i-1$).
- $\varphi_{A,B,k,i}$ is the fraction of the surface area of layer k that is occupied by molecules of A that covers B molecules trapped below the upper layer i ($2 \leq i \leq N$) that is not covered by any higher layer of adsorbate (with $1 \leq k \leq i-1$).
- $\varphi_{B,k,i}$ is the fraction of the surface area of layer k that is occupied by molecules of B, and, according to the assumptions of the model, covers the sublayer $k-1$ of adsorbate molecules of A trapped below the upper layer i

($2 \le i \le N$) that is not covered by any higher layer of adsorbate (with $1 \le k \le i-1$).
- C_A and C_B are the concentrations of compounds A and B in the mobile phase, respectively.
- q_A and q_B are the total concentrations of compounds A and B in the adsorbed phase, respectively.
- $k^a_{A,S}$ and $k^d_{A,S}$ are the rate constants of adsorption and desorption of compound A on the solid surface, respectively.
- $k^a_{B,S}$ and $k^d_{B,S}$ are the rate constants of adsorption and desorption of compound B on the solid surface, respectively.
- $k^a_{A,A}$ and $k^d_{A,A}$ are the rate constants of adsorption and desorption of compound A on any intermediate local layer of compound A made on the solid surface, respectively.
- $k^a_{B,A}$ and $k^d_{B,A}$ are the rate constants of adsorption and desorption of compound B on any intermediate local layer of compound A made on the solid surface, respectively.
- $k^a_{A,B}$ and $k^d_{A,B}$ are the rate constants of adsorption and desorption of compound A on any intermediate local layer of compound B made on the solid surface, respectively. These parameters are the only two additional rate constants introduced in the new kinetic model.

2.4.3. Combinations of parameters

- The ratios $b_{A,S} = k^a_{A,S}/k^d_{A,S}$ and $b_{A,A} = k^a_{A,A}/k^d_{A,A}$ are the equilibrium constants of adsorption of compound A onto the free solid surface and onto a layer made of molecules of A, respectively.
- The ratios $b_{B,S} = k^a_{B,S}/k^d_{B,S}$ and $b_{B,A} = k^a_{B,A}/k^d_{B,A}$ are the equilibrium constants of adsorption of compound B onto the free solid surface and onto a layer made of molecules of A, respectively.
- The ratio $b_{A,B} = k^a_{A,B}/k^d_{A,B}$ is the equilibrium constant of adsorption of compound A onto a layer made of molecules of B.
- $r_{X,Y} = k^d_{X,Y}/k^d_{Y,S}$, with {X, Y}={A, A}, {A, B} or {B, A}.
- $t_{X,Y} = k^d_{X,Y}/k^d_{A,A}$, with {X, Y}={A, B} or {B, A}.
- $K_1 = 1 + b_{A,B} r_{A,B} C_A$.
- $K_2 = 1 + b_{A,B} t_{A,B} C_A / t_{B,A}$.
- $K_L = b_{A,B}/b_{A,A}$.
- $K_S = b_{B,S} b_{A,A} / b_{B,A} b_{A,S}$.
- $\alpha = 1/(1 + b_{A,B} b_{B,A} C_B / b_{A,A})$.

2.4.4. Strategy followed to derive the competitive isotherm

We will first write the $2N+1$ surface fractions of the adsorbent surface that are occupied by the free adsorbent surface and by either component A or B adsorbed on the top of each of the $1 \le i \le N$ layers of the adsorbed phase in contact with the liquid mobile phase. Then, we write phase equilibrium as:

$$\frac{\partial \theta_{A,i}}{\partial t} = 0 \tag{9-iA}$$

$$\frac{\partial \theta_{B,i}}{\partial t} = 0, \quad \text{with } 1 \le i \le N \tag{9-iB}$$

Since there are N layers, this gives $2N$ equations. The normalization condition of the surface fractions gives the last equation:

$$\theta_0 + \sum_{i=1}^{i=N} [\theta_{A,i} + \theta_{B,i}] = \theta_0 + \sum_{i=1}^{i=N} [\theta_{A,A,i} + \theta_{A,B,i} + \theta_{B,i}] = 1 \tag{10}$$

The difficulty in solving this system of equations resides in the fact that the proportion α_i of molecules of A adsorbed on molecules of A in the ith upper layer is, a priori, unknown ($2 \le i \le N$), which makes $3N$ unknown for only $2N+1$ equations. A first guess will have to be done if one wants to solve the system of $2N+1$ equations. The guess assumes that the α_i values are all equal to the α value that will be assessed in the next section. Then the number of unknowns drops from $3N$ to $2N+1$, the exact number of equations provided by the kinetic equations and the surface fraction normalization equation.

Second, once the $\theta A, A, i$, $\theta_{A,B,i}$ and $\theta_{B,i}$ are known, the suface fractions φ of the molecules of A and B that are trapped below the upper layers i have to be derived in order to calculate the total amounts adsorbed. For any layer i that is not covered, there are $3(i-1)-1$ unknown φ variables. In order to derive them, we will write the equation stating kinetic "equilibrium" between two successive internal layers (i.e., between layers k and $k+1$ with $1 \le k \le i-1$). These equilibria describe the exchanges between a B molecule and an A molecule belonging to two neighboring layers. This exchange may lead to a local change of the interaction configuration in the adsorbed phase so that the equilibrium constant is not necessarily unity (see Fig. 2a–d). If the exchange occurs between the layer k and the layer $k+1$, the layer $k+2$ should also be considered in the calculation of the equilibrium constant. From the adsorbent surface ($k=1$) up to the highest layer involved ($k = i-1$), there are $i-1$ equilibrium relationships of this kind. The activity coefficients of the solutes were assumed to be equal to their respective fractional surface coverage:

$$K(\text{SABA} \leftrightarrow \text{SBAA}) = K^i_{1\leftrightarrow 2} = K_S = \frac{\varphi_{A,A,3,i}\varphi^2_{A,B,2,i}}{\varphi_{A,1,i}\varphi^2_{A,B,3,i}} \tag{11-1}$$

$$K(\text{AABA} \leftrightarrow \text{ABAA}) = K^i_{2\leftrightarrow 3} = 1 = \frac{\varphi_{A,A,4,i}\varphi^2_{A,B,3,i}}{\varphi_{A,A,2,i}\varphi^2_{A,B,4,i}} \tag{11-2}$$

...

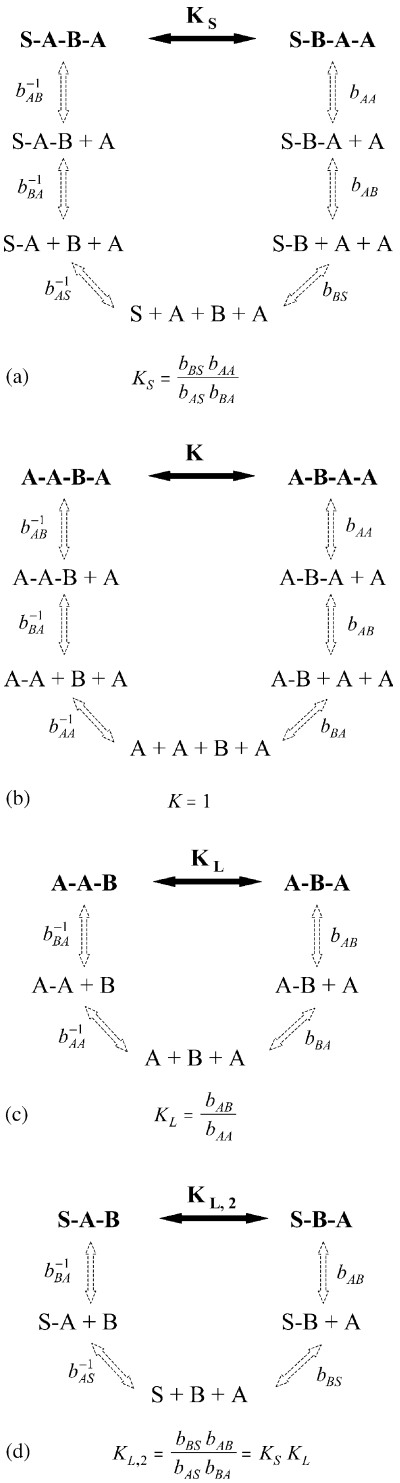

Fig. 2. (a) Determination of the equilibrium constant K_S, associated to the exchange of a molecule of A and B between the first ($k = 1$) and the second ($k = 2$) layers. (b) Determination of the equilibrium constant K associated to the exchange of a molecule of A and B between two neighboring layers ($k \leftrightarrow k+1$) in the adsorbed phase. (c) Determination of the equilibrium constant associated to the exchange of a molecule of A and a molecule of B between the last but one ($k = i-1$) and the last ($k = i$) layers. (d) Same as c) for $i = 2$.

$$K(\mathrm{AABA} \leftrightarrow \mathrm{ABAA}) = K^i_{k\leftrightarrow k+1} = 1 = \frac{\varphi_{\mathrm{A,A},k+2,i}\varphi^2_{\mathrm{A,B},k+1,i}}{\varphi_{\mathrm{A,A},k,i}\varphi^2_{\mathrm{A,B},k+2,i}} \quad (11\text{-k})$$

...

$$K(\mathrm{AABA} \leftrightarrow \mathrm{ABAA}) = K^i_{i-2\leftrightarrow i-1} = 1 = \frac{\theta_{\mathrm{A,A},i}\varphi^2_{\mathrm{A,B},i-1,i}}{\varphi_{\mathrm{A,A},i-2,i}\theta^2_{\mathrm{A,B},i}} \quad (11\text{-(i-2)})$$

$$K(\mathrm{AABL} \leftrightarrow \mathrm{ABAL}) = K^i_{i-1\leftrightarrow i} = K_{\mathrm{L}} = \frac{(1-\alpha_i)^2\theta^2_{\mathrm{A},i}}{\varphi_{\mathrm{A,A},i-1,i}\theta_{\mathrm{B},i}} \quad (11\text{-(i-1)})$$

where S represents the adsorbent surface area and L the liquid phase in contact with the adsorbed phase.

In addition to these equations, there are $i-1$ equations coming from the normalization of all of the sublayers' fractions of surface area of the upper layer i:

$$\varphi_{\mathrm{A,A},k,i} + \varphi_{\mathrm{A,B},k,i} + \varphi_{\mathrm{B},k,i} = \theta_{\mathrm{A},i} + \theta_{\mathrm{B},i} \quad (12\text{-}\{\mathrm{k,i}\})$$

and finally there are $i-1$ other equations arising from the assumption made in the model (i.e., that the B molecules can not adsorb on themselves but only on molecules of A):

$$\varphi_{\mathrm{B},k,i} = \varphi_{\mathrm{A,B},k+1,i} \quad (13\text{-}\{\mathrm{k,i}\})$$

This makes a total of $3(i-1)$ equations for only $3(i-1)-1$ φ unknowns. The Eq. (11-(i-2)) will be omitted at this stage because they involve α_i, which was already fixed by the initial guess.

Accordingly, this last equation provides a useful check of the validity of the initial guess α for the coefficients α_i. If the difference between α and α_i is large, the whole process will be repeated (resolution of the system of the $2N+1$ Eqs. (9) and (10)) from a new values α_i given by Eq. (11-(i-2)) until convergence is reached.

Finally, the total amounts of compounds A and B that are adsorbed at equilibrium can be calculated by the double sum (first the sum on the level i of the top layer and second the sum on the level k of the sublayers) of all the fractions of surface area and by multiplying them by the saturation capacity of the corresponding compound:

$$q_{\mathrm{A}} = q_{\mathrm{s,A}}\left[\sum_{i=1}^{i=N}\left(\theta_{\mathrm{A},i} + \sum_{k=1}^{k=i-1}\varphi_{\mathrm{A,A},k,i} + \varphi_{\mathrm{A,B},k,i}\right)\right] \quad (14\text{-A})$$

$$q_{\mathrm{B}} = q_{\mathrm{s,B}}\left[\sum_{i=1}^{i=N}\left(\theta_{\mathrm{B},i} + \sum_{k=1}^{k=i-1}\varphi_{\mathrm{B},k,i}\right)\right] \quad (14\text{-B})$$

2.4.5. Development of the system of the (2N + 1) Eqs. (9) and (10)

2.4.5.1. Adsorption–desorption equilibrium on the first layer. There are three ways for the surface fraction $\theta_{\mathrm{A},1}$ to increase:

- when A adsorbs on the free surface θ_0,
- when A desorbs from the second layer on a molecule of A, and
- when B desorbs from the second layer on a molecule of A.

Similarly, there are three ways that the surface fraction $\theta_{A,1}$ may decrease:

- when A adsorbs on the first layer of A molecules,
- when B adsorbs on the first layer of A molecules, and
- when A desorbs from the first layer.

These different processes may be written as follows:

$$k^{a}_{A,S}C_A\theta_0 + \alpha_2 k^{d}_{A,A}\theta_{A,2} + k^{d}_{B,A}\theta_{B,2} - (k^{a}_{A,A}C_A + k^{a}_{B,A}C_B + k^{d}_{A,S})\theta_{A,1} = 0 \quad (15\text{-}1A)$$

For compound B, the situation is somewhat simpler because B may not adsorb on itself (model assumption III). The surface fraction $\theta_{B,1}$ increases:

- when B adsorbs on the free surface θ_0, and
- when A desorbs from the second layer on a molecule B.

The surface fraction $\theta_{B,1}$ decreases:

- when B desorbs from the first layer, and
- when A adsorbs on molecule B in the first layer.

Hence:

$$k^{a}_{B,S}C_B\theta_0 + (1-\alpha_2)k^{d}_{A,B}\theta_{A,2} - k^{d}_{B,S}\theta_{B,1} - k^{a}_{A,B}C_A\theta_{B,1} = 0 \quad (15\text{-}1B)$$

2.4.5.2. Adsorption–desorption equilibrium on the second layer. By iteration to the second layer, we obtain a similar pair of equations for the variation of the surface fractions $\theta_{A,2}$ and $\theta_{B,2}$:

$$k^{a}_{A,A}C_A\theta_{A,1} + k^{a}_{A,B}C_A\theta_{B,1} + \alpha_3 k^{d}_{A,A}\theta_{A,3} + k^{d}_{B,A}\theta_{B,3} - (k^{a}_{A,A}C_A + k^{a}_{B,A}C_B + \alpha_2 k^{d}_{A,A} + (1-\alpha_2)k^{d}_{A,B})\theta_{A,2} = 0 \quad (15\text{-}2A)$$

$$k^{a}_{B,A}C_B\theta_{A,1} + (1-\alpha_3)k^{d}_{A,B}\theta_{A,3} - (k^{a}_{A,B}C_A + k^{d}_{B,A})\theta_{B,2} = 0 \quad (15\text{-}2B)$$

This result is easily generalized to the cases of any layer from 3 to N.

2.4.5.3. Adsorption–desorption equilibrium on layer i. The following equations are obtained:

$$k^{a}_{A,A}C_A\theta_{A,i-1} + k^{a}_{A,B}C_A\theta_{B,i-1} + \alpha_{i+1}k^{d}_{A,A}\theta_{A,i+1} + k^{d}_{B,A}\theta_{B,i+1} - (k^{a}_{A,A}C_A + k^{a}_{B,A}C_B + \alpha_i k^{d}_{A,A} + (1-\alpha_i)k^{d}_{A,B})\theta_{A,i} = 0 \quad (15\text{-}iA)$$

$$k^{a}_{B,A}C_B\theta_{A,i-1} + (1-\alpha_{i+1})k^{d}_{A,B}\theta_{A,i+1} - (k^{a}_{A,B}C_A + k^{d}_{B,A})\theta_{B,i} = 0 \quad (15\text{-}iB)$$

2.4.5.4. Adsorption–desorption equilibrium on layer N. The following equations are obtained:

$$k^{a}_{A,A}C_A\theta_{A,N-1} + k^{a}_{A,B}C_A\theta_{B,N-1} - (\alpha_N k^{d}_{A,A} + (1-\alpha_N)k^{d}_{A,B})\theta_{A,N} = 0 \quad (15\text{-}NA)$$

$$k^{a}_{B,A}C_B\theta_{A,N-1} - k^{d}_{B,A}\theta_{B,N} = 0 \quad (15\text{-}NB)$$

2.4.5.5. System of equations. The last equation of the system of $2N+1$ equations is obtained by writing that the sum of the free surface fraction θ_0 and of the fractions of the surface occupied by molecules of A ($\theta_{A,i}$) and B($\theta_{B,i}$) and that are not covered by any higher layer, is 1 (Eq. (10)). We now dispose of a system of $2N+1$ equations but this system contains $3N$ unknowns (θ_0, $\theta_{A,1}$, $\theta_{B,1}$ and $\theta_{A,i}$, α_i, $\theta_{B,i}$ for $2 \leq i \leq N$). As aforementioned, $N-1$ equations are still missing to complete a determined system. This situation arises because we do not know the fraction α_i of A molecules adsorbed on other A molecules in the ith uncovered layer. An initial guess must be made. Let us consider a fictitious heterogeneous adsorbent surface made only of molecules of A and B in equilibrium with a solution of molecules of both A and B (with no underlying or exposed adsorbent). It would be much like the surface of a mixed A + B solid. Then, α or the fraction of A molecules adsorbed on A molecules is easily derived from the three simultaneous equilibria that may take place in this hypothetical system and which describe the three possible exchanges between the adsorbed and the mobile phases:

$$\equiv A + A \Leftrightarrow \equiv AA \qquad K = b_{A,A} \quad (16\text{-}AA)$$

$$\equiv A + B \Leftrightarrow \equiv AB \qquad K = b_{B,A} \quad (16\text{-}BA)$$

$$\equiv B + A \Leftrightarrow \equiv BA \qquad K = b_{A,B} \quad (16\text{-}AB)$$

Defining

$$\alpha = \frac{[\equiv AA]}{[\equiv AA] + [\equiv BA]} \quad (17)$$

and since $[\equiv A] = [\equiv AA] + [\equiv BA]$ and $[\equiv B] = [\equiv AB]$, we have

$$\alpha = \frac{1}{(1 + b_{A,B}b_{B,A}C_B)/(b_{A,A})} \quad (18)$$

We will assume as the first guess to solve the equation system that all the α_i values are equal to α. This assumption gives $N-1$ additional equations:

$$\alpha_2 = \alpha_3 = \cdots = \alpha_i = \cdots = \alpha_N = \alpha \quad (19\text{-}i)$$

This simplification, based on a physical approximation that cannot describe correctly the actual adsorption system, can serve as an acceptable initial guess to begin an iteration process and solve the whole problem. The number of unknowns in the system is now equal to the number of equations and the system can be solved.

2.4.6. Resolution of the system of equation

Using the definitions and notations defined earlier and eliminating the surface fractions of B by substituting Eq. (15-iB) into Eq. (15-iA), the system of $2N+1$ equations just derived can be rewritten as follows.

2.4.6.1. For the first layer.

$$\left[1 + r_{A,A}b_{A,A}C_A + r_{B,A}b_{B,A}C_B\left(\frac{K_2-1}{K_2}\right)\right]\theta_{A,1} = b_{A,S}C_A\theta_0 + \alpha_2 r_{A,A}\theta_{A,2} + \frac{(1-\alpha_3)r_{B,A}t_{A,B}}{K_2 t_{B,A}}\theta_{A,3} \quad (20\text{-}1A)$$

2.4.6.2. For the second layer. Following the same procedure for the similar relationships for the third and second layers, we obtain:

$$\left[\alpha_2 + (1-\alpha_2)t_{A,B} + b_{A,A}C_A + t_{B,A}b_{B,A}C_B\left(\frac{K_2-1}{K_2}\right) - \frac{(1-\alpha_2)t_{A,B}r_{A,B}b_{A,B}C_A}{K_1}\right]\theta_{A,2} = \frac{t_{A,B}b_{A,B}b_{B,S}C_AC_B}{K_1}\theta_0 + b_{A,A}C_A\theta_{A,1} + \alpha_3\theta_{A,3} + (1-\alpha_4)\frac{t_{A,B}}{K_2}\theta_{A,4} \quad (20\text{-}2A)$$

2.4.6.3. For the ith layer. For the subsequent layers i ($3 \geq i \geq N-2$), we obtain:

$$\left[\alpha_i + (1-\alpha_i)t_{A,B} + b_{A,A}C_A + t_{B,A}b_{B,A}C_B\left(\frac{K_2-1}{K_2}\right) - \frac{(1-\alpha_i)t_{A,B}^2 b_{A,B}C_A}{K_2 t_{B,A}}\right]\theta_{A,i} = \frac{t_{A,B}b_{A,B}b_{B,A}C_AC_B}{K_2}\theta_{A,i-2} + b_{A,A}C_A\theta_{A,i-1} + \alpha_{i+1}\theta_{A,i+1} + (1-\alpha_{i+2})\frac{t_{A,B}}{K_2}\theta_{A,i+2} \quad (20\text{-}iA)$$

2.4.6.4. For the $(N-1)$th layer.

$$\left[\alpha_{N-1} + (1-\alpha_{N-1})t_{A,B} + b_{A,A}C_A - \frac{(1-\alpha_{N-1})t_{A,B}^2 b_{A,B}C_A}{K_2 t_{B,A}}\right]\theta_{A,N-1} = \frac{t_{A,B}b_{A,B}b_{B,A}C_AC_B}{K_2}\theta_{A,N-3} + b_{A,A}C_A\theta_{A,N-2} + \alpha_N\theta_{A,N} \quad (20\text{-(N-1)A})$$

2.4.6.5. For the Nth layer.

$$\left[\alpha_N + (1-\alpha_N)t_{A,B} - \frac{(1-\alpha_N)t_{A,B}^2 b_{A,B}C_A}{K_2 t_{B,A}}\right]\theta_{A,N} = \frac{t_{A,B}b_{A,B}b_{B,A}C_AC_B}{K_2}\theta_{A,N-2} + b_{A,A}C_A\theta_{A,N-1} \quad (20\text{-NA})$$

2.4.6.6. Fractional surface coverage of B. These surface coverages, $\theta_{B,i}$, can be derived according to Eq. (15-iB):

$$\theta_{B,1} = \frac{b_{B,S}C_B}{K_1}\theta_0 + (1-\alpha_2)\frac{r_{A,B}}{K_1}\theta_{A,2} \quad (20\text{-}1B)$$

...

$$\theta_{B,i} = \frac{b_{B,A}C_B}{K_2}\theta_{A,i-1} + (1-\alpha_{i+1})\frac{t_{A,B}}{t_{B,A}K_2}\theta_{A,i+1} \quad (20\text{-}iB)$$

...

$$\theta_{B,N} = b_{B,A}C_B\theta_{A,N-1} \quad (20\text{-NB})$$

2.4.6.7. Fractional surface coverage of A. Starting from layer N and substituting Eq. (20-NA) into Eq. (20-(N-1)A), each surface fraction $\theta_{A,i}$ can be successively written under the form:

$$\gamma_i\theta_{A,i} = \beta_{i,1}\theta_{A,i-1} + \beta_{i,2}\theta_{A,i-2} \quad (21\text{-}iA)$$

Eq. (10) provides the free surface fraction θ_0, allowing the calculation of the surface fractions of molecules A and B in the upper layer i (i.e., of $\theta_{A,A,i}$, $\theta_{A,B,i}$, and $\theta_{B,i}$ for $2 \leq i \leq N$, as well as of $\theta_{A,1}$ and $\theta_{B,1}$ in the monolayer in contact with the adsorbent).

2.4.7. Determination of the internal fractional surface coverages

The amount of A and B trapped below these top layers (according to the description of internal piled layers shown in Fig. 1) must be calculated to obtain the total amount adsorbed. For instance, let us consider the upper layer, i. $\varphi_{A,A,k,i}$, $\varphi_{A,B,k,i}$ and $\varphi_{B,k,i}$ are the fractional surface coverages in the adsorbed phase in the kth sublayer ($1 \leq k \leq i-1$). There are $3(i-1)-1$ unknowns since only two variables are defined for $k=1$ ($\varphi_{A,1,i}$ and $\varphi_{B,1,i}$), so we need as many independent equations relating these coverages in order to derive them.

First, we write the relationships stating equilibrium in the adsorbed phase regarding the exchange of a B for an A molecule between two consecutive sublayers ($k \leftrightarrow k+1$). This gives the following $i-2$ equations:

$$\theta_{A,A,i}\varphi_{A,B,i-1,i}^2 = \theta_{A,B,i}^2\varphi_{A,A,i-2,i} \quad (22\text{-}\{i\text{-}2,i\})$$

$$\varphi_{A,A,i-1,i}\varphi_{A,B,i-2,i}^2 = \varphi_{A,B,i-1,i}^2\varphi_{A,A,i-3,i} \quad (22\text{-}\{i\text{-}3,i\})$$

...

$$\varphi_{A,A,k,i}\varphi^2_{A,B,k-1,i} = \varphi^2_{A,B,k,i}\varphi_{A,A,k-2,i} \quad (22\text{-}\{k\text{-}2,i\})$$

...

$$\varphi_{A,A,4,i}\varphi^2_{A,B,3,i} = \varphi^2_{A,B,4,i}\varphi_{A,A,2,i} \quad (22\text{-}\{2,i\})$$

$$\varphi_{A,A,3,i}\varphi^2_{A,B,2,i} = K_S\varphi^2_{A,B,3,i}\varphi_{A,1,i} \quad (22\text{-}\{1,i\})$$

From the assumption made in the model that a molecule of B never adsorbs on a molecule of B (assumption III), the interaction configuration in the adsorbed phase remains unchanged when a B molecule is exchanged for an A molecule between two neighboring layers (e.g., from layer k to layer $k+1$ for $2 \geq k \geq i-2$) so the equilibrium constant is unity (see Fig. 2b). The converse situation is different, as shown in Fig. 2a, when a B molecule is exchanged for an A molecule between layers 1 and 2 (or between layers $i-1$ and i in Fig. 2c and d), see later. A change in the interaction configuration takes place in the adsorbed phase. By decomposing the exchange process into fictitious intermediate steps it is easily demonstrated that (see Fig. 2):

$$K_S = \frac{b_{B,S}b_{A,A}}{b_{B,A}b_{A,S}} \quad (23)$$

Second, we have $i-1$ normalization equations that must be fulfilled:

$$\varphi_{A,A,i-1,i} + \varphi_{A,B,i-1,i} + \varphi_{B,i-1,i} = \theta_i \quad (24\text{-}\{i\text{-}1,i\})$$

...

$$\varphi_{A,A,k,i} + \varphi_{A,B,k,i} + \varphi_{B,k,i} = \theta_i \quad (24\text{-}\{k,i\})$$

...

$$\varphi_{A,A,2,i} + \varphi_{A,B,2,i} + \varphi_{B,k,i} = \theta_i \quad (24\text{-}\{2,i\})$$

$$\varphi_{A,1,i} + \varphi_{B,1,i} = \theta_i \quad (24\text{-}\{1,i\})$$

where $\theta_i = \theta_{A,A,i} + \theta_{A,B,i} + \theta_{B,i}$.

Finally, the assumption that B molecules adsorb only on A molecules but not on other B molecules give $i-1$ equations

$$\varphi_{B,i-1,i} = \theta_{A,B,i} \quad (25\text{-}\{i\text{-}1,i\})$$

...

$$\varphi_{B,k,i} = \varphi_{A,B,k+1,i} \quad (25\text{-}\{k,i\})$$

...

$$\varphi_{B,1,i} = \varphi_{A,B,2,i} \quad (25\text{-}\{1,i\})$$

This makes a total of $(i-2)+(i-1)+(i-1) = 3(i-1)-1$ equations that are required to solve the system of $3(i-1)-1$ unknowns.

Note that we decided to omit the exchange B $\leftrightarrow$ A between layers $i-1$ and i. Their inclusion would lead to the exact solution for the value of α_i but also to $N-1$ additional constraints. But we already made an assumption regarding the values of the $N-1$ α_i. They are all supposed to be equal to α as aforementioned. This first guess for the α_i values has the advantage of decoupling the Eqs. (9) and (10) from those used to derive the φ surface fraction areas (Eqs. 22-{k-2,i}, 24-{k,i} and 25-{k,i}). However, this particular exchange exists and our solution must, eventually be consistent with our initial estimate, at least within a certain agreement criterion. The corresponding relationship and the associated equilibrium constant K_L are (see Fig. 2c):

$$(1-\alpha_i)^2\theta^2_{A,i} = K_L\theta_{B,i}\varphi_{A,A,i-1,i} \quad (26\text{-}\{i\text{-}1,i\})$$

If $i = 2$ then it is easily shown that this same equation becomes (see Fig. 2d):

$$(1-\alpha_2)^2\theta^2_{A,2} = K_S K_L\theta_{B,2}\varphi_{A,1,2} \quad (26\text{-}\{1,2\})$$

The first guess chosen for the α_i values ($\forall i, \alpha_i = \alpha$) will be tested by calculating the following relative errors:

$$\frac{\Delta\alpha_i}{\alpha_i} = \frac{|\alpha - 1 + (\sqrt{K_L\theta_{B,i}\varphi_{A,A,i-1,i}}/\theta_{A,i})|}{1 - (\sqrt{K_L\theta_{B,i}\varphi_{A,A,i-1,i}}/\theta_{A,i})} \quad (27)$$

If this error is larger than 0.1%, the α_i values will be reinitialized to the new guess given by equation 26-{i-1,i} and the whole procedure will be repeated until convergence for all α_i values.

An example of application is given in the appendix. It shows the derivation procedure in the particular case of an adsorbed phase made of five layers.

2.5. Numerical calculations

In all the numerical calculations applied to derive the final theoretical isotherm data, the multilayer adsorbed system was limited to five layers (see further Section 4.3). The concentration C_A and C_B in the mobile phase were fixed to arbitrary values. The values of the parameters listed in Section 2.4.3. (single-component isotherm parameters, $b_{A,B}$, $r_{X,Y}$, $t_{X,Y}$, K_1, K_2, K_L, K_S and α) were fixed. The numerical values of the parameters γ_i, $\beta_{i,1}$ and $\beta_{i,2}$ in Eq. (21-iA) can then be calculated from Eqs. (28-{i,0}), (28-{i,1}) and (28-{i,2}) described in the Appendix A. The system of $2N+1$ equations (Eqs. (10), (20-iB) and (21-iA) associated to equilibrium of the upper layers i) is solved numerically by using the SOLVER tool option available in the EXCEL spreadsheet. The solutions provide the initial set of fractional surfaces $\theta_{A,A,i}$, $\theta_{A,B,i}$ and $\theta_{B,i}$ of the five upper layers as well as the fractional surface coverage of the free surface θ_0.

In a second step (see in the Appendix A), the numerical solutions (also accomplished by using the SOLVER tool in EXCEL) of the Eqs. (32), (36) and (37) allow the determination of all the fractional surface coverages associated with the layers of molecules trapped below the upper layers with respect to the relations given by Eq.(22-{k-2,i}) (system equilibrium), Eq.(24-{k,i}) (surface normalization condition) and Eq.(25-{k,i}) (model assumption #III). Eq. (26-{i-1,i}) deliver finally a new guess for the α_i values. According to Eq. (27) and the convergence criterium of 0.1% for all the α_i values, the numerical resolution of the same system of $2N+1$ equation is repeated or not.

The final amount adsorbed (Eqs. (14-A) and (14-B)) can be calculated once the convergence of all the α_i coefficients has been reached.

3. Experimental

3.1. Chemicals

The mobile phase used in this work was a mixture of HPLC grade water and methanol (62% methanol, 38% water, v/v), both purchased from Fisher Scientific (Fair Lawn, NJ, USA). The same mobile phase was used for the determination of the single-component adsorption isotherm data and for the recording of large size band profiles of the two single components and of some of their binary mixtures. The solvents used to prepare the mobile phase were filtered before use on an SFCA filter membrane, 0.2 μm pore size (Suwannee, GA, USA).

The solutes used were uracil, 4-*tert*-butylphenol, and ethylbenzoate. All were obtained from Aldrich (Milwaukee, WI, USA).

3.2. Materials

A manufacturer-packed, 250 mm × 4.6 mm Kromasil column was used (Eka Nobel, Bohus, Sweden, EU). This column was packed with a C_{18}-bonded, endcapped, porous silica. This column (Column #E6021) was one of the lot of ten columns previously used by Kele [25], Gritti [26] and Felinger [27] for their study of the reproducibility of the chromatographic properties of RPLC columns under linear and non-linear conditions. The main characteristics of the bare porous silica and of the packing material used are summarized in Table 1.

The hold-up time of this column was derived from the retention time of uracil injections. With a mobile phase composition of 62/38, the elution time of uracil is nearly the same as that of pure methanol or sodium nitrate. The product of this time and the mobile phase flow rate gives an excellent estimate of the column void volume. The void volume of the column and its total porosity ϵ_T in 62/38 (v/v) methanol/water mobile phase are 2.40 cm^3 and 0.577, respectively.

Table 1
Physico-chemical properties of the packed Kromasil-C_{18} (Eka) #E6021 column

Particle size (μm)	5.98
Particle size distribution (90:10, % ratio)	1.44
Pore size (Å)	112
Pore volume (ml/g)	0.88
Surface area (m^2/g)	314
Na, Al, Fe content (ppm)	11, <10, <10
Particule shape	Spherical
Total carbon (%)	20.0
Surface coverage (μmol/m^2)	3.59
Endcapping	Yes

3.3. Apparatus

The competitive isotherm data were acquired using a Hewlett-Packard (Palo Alto, CA, USA) HP 1090 liquid chromatograph. This instrument includes a multi-solvent delivery system (tank volume, 1 dm^3 each), an auto-sampler with a 25 μl loop, a diode-array UV-detector, a column thermostat and a computer data acquisition station. Compressed nitrogen and helium bottles (National Welders, Charlotte, NC, USA) are connected to the instrument to allow the continuous operation of the pump and auto- sampler and solvent sparging. The extra-column volumes are 0.058 ml and 0.90 ml as measured from the auto-sampler and from the pump system, respectively, to the column inlet. All the retention data were corrected for this contribution. The flow-rate accuracy was controlled by pumping the pure mobile phase at 23 °C and 1 ml/min during 50 min, from each pump head, successively, into a volumetric glass of 50 ml. A relative error of less than 0.4% was obtained so that we can estimate the long- term accuracy of the flow-rate at 4 μl/min at flow rates around 1 ml/min. All measurements were carried out at a constant temperature of 23 °C, fixed by the laboratory air-conditioner. The daily variation of the ambient temperature never exceeded 1 °C.

3.4. Competitive isotherm measurements by frontal analysis (FA)

One pump of the HPLC instrument was used to deliver a stream of the pure mobile phase, the second pump, a stream of the concentrated solution of the compound(s) studied in the same mobile phase. The concentration of the compound(s) studied in each FA run is determined by the concentration of the mother sample solution and the flow rate fractions delivered by the two pumps. The breakthrough curves are recorded successively, at a flow rate of 1 cm^3/min, with a sufficiently long time delay between each breakthrough curve to allow for the reequilibration of the column with the pure mobile phase. The injection time of the sample varied between 5 and 12 min in order to reach a stable plateau for both components at the column outlet. The signals of 4-*tert*-butyl phenol and ethylbenzoate were both detected with the UV detector at 295 nm.

For the injected solutions whose concentration ranged between 1 and 19 g/l, it was assumed that the breakthrough profile of each single-component solution exhibits a front shock-layer so that Eqs. (1) and (2) were used to calculate the amounts adsorbed. On the other hand, for the mixture solution of 4-*tert*-butyl phenol and ethylbenzoate at 25 g/l each, the concentration of each compound in the elution profile had to be determined by fraction collection and analysis because the front part of the profile of ethylbenzoate was clearly not a shock layer and, therefore, Eqs. (1) and (2) do not apply in this case. The individual band profiles were measured accurately by collecting 20 fractions of 250 μl (i.e., 18 droplets each), at a constant flow rate of

1 ml/min, between the elution times of 11.6 and 16.6 min. Ten microliter aliquotes of each fractions were then injected into the same column, using a 70/30 (v/v) methanol/water mixture as the mobile phase. After a preliminary calibration, the measurement of the areas of the two separated peaks, recorded at 285 nm, allowed the determination of the concentration of each individual component in each collected fraction. The individual and total band profiles in the mixed zone were reconstituted by assigning a time to each fraction. This time is determined by the actual collection time minus the sum of the times needed for the mobile phase to percolate through the extra-column volume (55 s at 1 ml/min) and through the capillary connecting the detector cell and the collector vials (10 s at 1 ml/min).

4. Results and discussion

4.1. Competitive binary adsorption data. Competitive breakthrough profiles and isotherms

Fig. 3a shows eight breakthrough curves recorded at 295 nm for the binary, equimolar mixture of ethylbenzoate and 4-*tert*-butylphenol. The adsorbed amounts are easily calculated using Eqs. (1) and (2), from the lowest concentration 1–19 g/l, provided that the calibration curve of the first component is known, allowing the determination of the height of the intermediate plateau concentration. These equations provide accurate estimates of the amounts of each compound adsorbed at equilibrium because the band profiles of both components have a front shock, hence of the competitive isotherms for the binary mixture studied (Fig. 4).

It is noteworthy that, while the front shock of 4-*tert*-butylphenol is eluted after that of ethylbenzoate at low concentrations, it is eluted before it at high concentrations. This result was expected because it had been reported earlier that the single-component isotherms of these two compounds intersect, so that the chord of the isotherm of 4-*tert*-butylphenol is higher than that of ethylbenzoate at low concentrations and lower at high concentrations [18]. So, it is not surprising to observe the same phenomenon for the competitive isotherm (Fig. 4). The intersection of the two isotherms Is observed for a concentration of about 6.25 g/l which is also the one for which the breakthrough curve of the mixture exhibits only one front shock instead of two at, e.g., 4 and 10 g/l.

A far more surprising result is that the competitive isotherm of 4-*tert*-butylphenol is profoundly different from the single-component isotherm. The latter is well accounted for by the Langmuir model. The former is no longer convex upward but exhibits an inflection point at around 13 g/l. The competitive isotherm of this compound cannot be accounted for by the Langmuir isotherm model. The fact that it is an S-shaped isotherm of type II means that the presence of ethylbenzoate affects considerably the adsorption of 4-*tert*-butylphenol on octadecyl silica at high concentrations. This observation is confirmed by the most unusual shapes of the individual breakthrough fronts of the two components for a concentrated solution at 25 g/l of each compound. These profiles were determined by the analysis of twenty fractions collected during the elution of the breakthrough front (See Fig. 5). There is no displacement effect of the first eluted component: the plateau eluted between 10 and 11 min after injection is at a concentration significantly lower than that of the feed.

The rear diffuse profiles of the eight breakthrough experiments are shown in Fig. 3b. Their shapes are also most

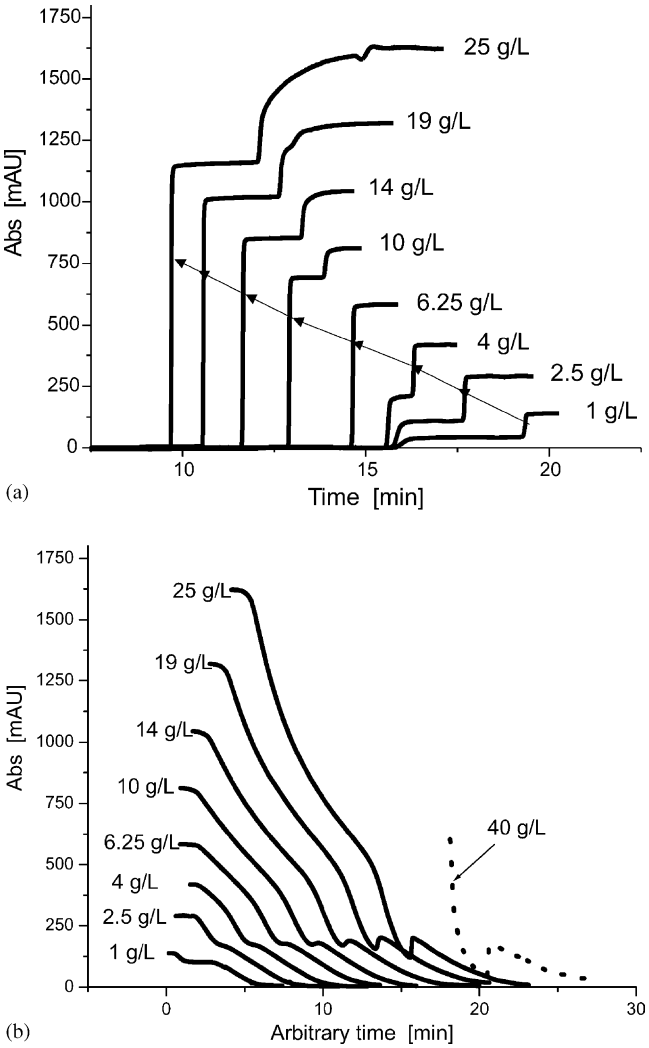

Fig. 3. (a) Experimental breakthrough curves of equimolar mixtures of ethylbenzoate and 4-*tert*-butylphenol for eight concentrations. The arrows locate the position of the front shock of 4-*tert*-butylphenol when the concentration increases. *Note:* First, the reversal position of the two shocks at the concentration of 6.25 g/l, where only one shock is observed. Second, note that the front shock of ethylbenzoate becomes a diffuse front beyond 14 g/l. (b) Same as (a) concerning the rear part of the FA breakthrough curves (thick lines). Note the progressive band splitting of 4-*tert*-butylphenol when the concentration increases. For a sake of comparison, the rear profile measured for a 40 g/l mixture is shown as a dotted line [19]. Remark the constant height of the isolated band, whatever the concentration applied.

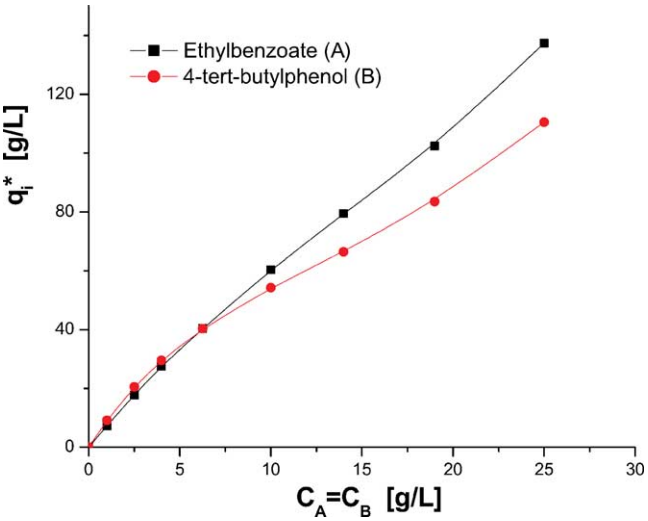

Fig. 4. Experimental competitive adsorption data measured by FA for mixtures of ethylbenzoate (squares) and 4-*tert*-butylphenol (circles) at eight concentrations (1, 2.5, 4, 6.25, 10, 14, 19 and 25 g/l). Note the reversal order of the amounts adsorbed at 6.25 g/l and the S-shaped isotherm for 4-*tert*-butylphenol whose single-component isotherm is strictly langmuirian.

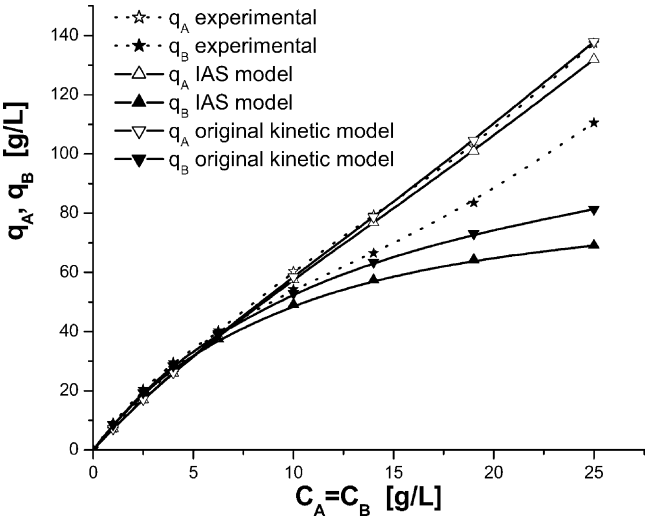

Fig. 6. Comparison between the competitive experimental isotherms of ethylbenzoate (empty stars, dotted line) and 4-*tert*-butylphenol (solid stars, dotted line) and the competitive isotherm models previously derived and given in Section 2.3 (up triangles: IAS model; down triangle: kinetic model). Note the good agreement at low concentrations but the strong discrepancies for 4-*tert*-butylphenol at high concentrations.

unusual. At low concentrations, below 6.25 g/l, the concentration at which the two isotherms intersect, the desorption profiles have a shape similar to the conventional ones, with an intermediate plateau for the more retained compound, i.e., 4-*tert*-butylphenol in this range. This plateau results from the tag-along effect [1]. Beyond this concentration, however, the intermediate plateau vanishes, a valley is formed and it becomes deeper with increasing solution concentration, as if a new band was progressively separated from the main part of the band profile. It is remarkable that the height of this new band remains constant (at about 1.3 g/l) and is independent of the feed concentration, from 6.25 to 40 g/l (see Fig. 3b). This phenomenon is confirmed by an observation reported previously [19] that the nearly complete separation of a third band of 4-*tert*-butylphenol takes place for a 0.5–2 ml sample of a 40 g/l solution and that the height of this band is also independent of the volume injected. This band splitting could be accounted for only qualitatively with the IAS and kinetic competitive isotherm models derived earlier (Section 2.3 and [19]). We compare now the experimental adsorption data to those predicted by the two theoretical models in order to study the limits of such models.

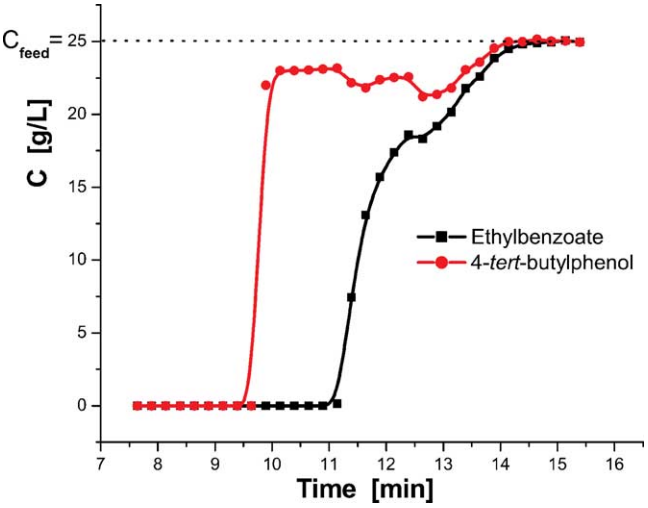

Fig. 5. Individual band profiles of the two-component breakthrough curve measured with a concentration in the feed of 25 g/l each for ethylbenzoate (squares) and 4-*tert*-butylphenol (circles). Note the complex shape of each band profile that forbids the use of Eqs. (1) and (2) to calculate the amounts adsorbed.

4.2. Comparison between the experimental adsorption data and the previous isotherm models

Fig. 6 compares the experimental isotherm data with those predicted by the two models derived earlier [19]. These two competitive models were consistent with the best single-component isotherms derived for ethylbenzoate and 4-*tert*-butylphenol, the Langmuir and the BET single-component isotherms, respectively. The parameters used for the competitive IAS model (Section 2.3.1) were those of the single-component isotherms derived by fitting the single-component isotherm data to this model [19], $q_{s,A} = 237.7$ g/l, $b_{A,S} = 0.03136$ l/g, $b_{A,A} = 0.0111$ l/g, $q_{s,B} = 164$ g/l, and $b_{B,S} = 0.05613$ l/g. The parameters used for the competitive kinetic model (Section 2.3.2) were also those derived by fitting the data to the single-component isotherm model. A last parameter of this second model, $b_{B,A}$, accounts for the adsorption of molecules of B on layers made of molecules of A. The value of this parameter

($b_{B,A} = 0.026$ l/g) was obtained by fitting the experimental band profiles of a binary mixture to those calculated with the isotherm. Results showed that both the kinetic and the IAS competitive models predict well the adsorption behavior of the two components at low and moderate concentrations, typically below the intersection point of the competitive isotherms of the two components. Beyond this concentration, discrepancies appear for both models, particularly for 4-*tert*-butylphenol. Both isotherms predict that the competitive isotherm for 4-*tert*-butylphenol remains convex upward at high concentrations while experimental data demonstrate that it is a S-shaped isotherm, first convex upward at low concentrations, then convex downward at high concentrations.

Accordingly, these two earlier models largely underestimate the amount of 4-*tert*-butylphenol adsorbed on the stationary phase at high concentrations. This demonstrates, first, that the mixture of ethylbenzoate and 4-*tert*-butylphenol cannot be considered as ideal in the adsorbed phase. Second, it shows that, although the kinetic model, which allows molecules of B to adsorb on layers made of molecules of A, gives a slightly better agreement with the experimental adsorption data, it remains unsatisfactory, probably also because of the nonideal behavior of the adsorbed phase. The large increase of the amount of 4-*tert*-butylphenol adsorbed at high concentrations, the corresponding change in the sign of the isotherm curvature, and the reversal of the elution order of the two components are not accounted for by this competitive model either. This is probably the reason why the kinetic approach did not lead to an accurate description of the overloaded band profiles of the two compounds studied and, more particularly, of the band splitting observed for 4-*tert*-butylphenol [19].

To take these results into account, we designed a new kinetic competitive isotherm based on the same set of assumptions but completed with an additional, physical assumption, that molecules of A could adsorb on a layer made of molecules of B. This will lead to larger amounts of A adsorbed at high concentrations.

4.3. Comparison between the experimental adsorption data and the new isotherm model

This competitive model uses the parameters of the single-component isotherms for the terms that are not products of both concentrations. The values of the other parameters are then estimated from the experimental adsorption data of the two components by parameter identification. Since a numerical solution is required for the calculation of the competitive adsorption data, a certain, finite number of layers must be assumed to calculate the theoretical competitive isotherm. For the sake of simplicity, we assumed this number of layers to be five. The multilayer BET isotherm (Eq. (5)) fits excellently the single-component adsorption data of ethylbenzoate in the range 0–40 g/l (See Fig. 7). It seemed useless to consider more layers, which would complicate the calculation of the amounts adsorbed for no apparent gain. Furthermore, this choice makes more physical sense than that of an infinite number of molecular layers which would hardly fit inside pores that have an average diameter of 110 Å. Under these conditions, the best single-component isotherm parameters for ethybenzoate are $q_{s,A} = 181.7$ g/l, $b_{A,S} = 0.04154$ l/g, $b_{A,A} = 0.01449$ l/g instead of $q_{s,A} = 237.7$ g/l, $b_{A,S} = 0.03136$ l/g, $b_{A,A} = 0.0111$ l/g when an infinite number of layers is assumed. Note that the saturation capacity of ethylbenzoate is now closer to that of 4-*tert*-butylphenol ($q_{s,B} = 164$ g/l), a result that seems to be far more acceptable since both low-molecular-weight compounds have exactly the same molar mass ($M_W = 150.2$ g/mol).

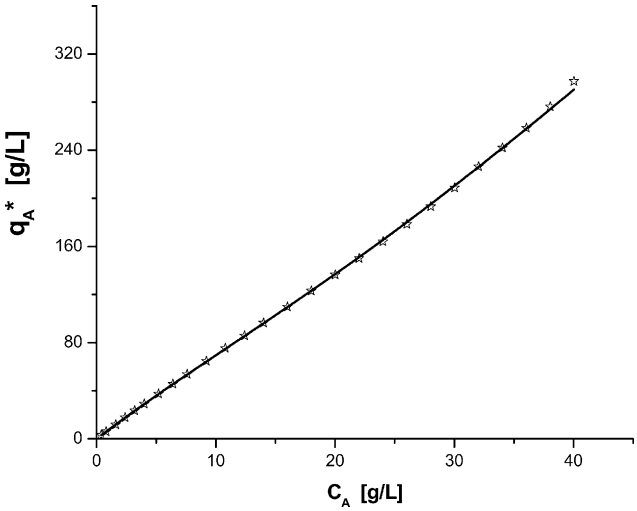

Fig. 7. Comparison between the single-component adsorption data (empty stars) of ethylbenzoate and the best multilayer BET model (solid line) assuming five piled layers.

This new model introduces in the competitive model two parameters, $b_{A,B}$ and $b_{B,A}$, to account for the interactions between the molecules of A and of B. These parameters cannot be derived from the single-component adsorption data but only from the competitive adsorption data. They were obtained by fitting to the model the experimental data acquired for the binary solution at 25 g/l. The amounts adsorbed were accurately measured by analyzing the 20 fractions collected during the five minutes that takes the elution of the breakthrough of the solution (see Fig. 5). This approach was preferred to the use of the amounts adsorbed at 19 g/l or 14 g/l (Fig. 4) because Eqs. (1) and (2) give only approximate values of the actual mass adsorbed for reasons aforementioned.

Finally, the model includes two other independent parameters, $t_{X,Y}$ and $r_{X,Y}$ (see definitions, Section 2.4.3.). These parameters are the ratios of two desorption rate constants. If we assume that the rates of adsorption of the molecules A and B, either on the adsorbent surface, S, or on any successive layer made of either adsorbate molecules are the same, we can write $t_{X,Y}$ and $r_{X,Y}$ as functions of the adsorption

constant $b_{X,Y}$. From the definitions in Section 2.4.3, we have:

$$t_{X,Y} = \frac{b_{B,A}}{b_{X,Y}} \quad (40)$$

$$r_{X,Y} = \frac{b_{Y,S}}{b_{X,Y}} \quad (41)$$

Then, the model contains only two variable parameters, $b_{A,B}$ and $b_{B,A}$. And we have also two equations to solve:

$$q_A\,(C_A = 25\,\text{g/l}, C_B = 25\,\text{g/l}, b_{A,B}, b_{B,A}) = q_{A,\text{exp}} \quad (42)$$

$$q_B\,(C_A = 25\,\text{g/l}, C_B = 25\,\text{g/l}, b_{A,B}, b_{B,A}) = q_{B,\text{exp}} \quad (43)$$

The best set of values derived from the numerical solutions of Eqs. 34 and 35 is $b_{A,B} = 0.0105$ l/g and $b_{B,A} = 0.0120$ l/g, with an accuracy of ± 0.0002 l/g. Fig. 8 compares the isotherm calculated from this set of parameters, in the range 0–25 g/l (lines), with the FA data (symbols). The agreement is much better than with the two previous models, particularly for the competitive isotherm of 4-*tert*-butylphenol at high concentrations. A slight difference is observed between the two sets of data regarding the intersection point of the two isotherms. It is predicted to take place at a concentration around 9 g/l instead of an experimental value of 6.25 g/l derived from the retention times of the front shocks of the two breakthrough curves (using Eqs. (1) and (2)). Nevertheless, the shapes of the two isotherms are now consistent with that of the experimental data, that is with a S-shape isotherm. For instance, Fig. 9 shows that the slope of the isotherm chord of the 4-*tert*-butylphenol isotherm strongly decreases with increasing concentration at low concentrations, reaches a minimum, and increases beyond 25 g/l. This is the direct consequence of the possibility for ethylbenzoate molecules to adsorb on layers made of molecules of B, which in turn, can adsorb on layers of molecules of A. This suggests that a synergetic adsorption phenomenon takes place in the studied system.

Finally, a plot of the evolution of the convergent α_i values (see Sections 2.4.2 and 2.4.3, and Eqs. (11), (13) and (15)) for concentrations ranging between 0 and 40 g/l and for two to five layers is shown in Fig. 10. Except for the highest

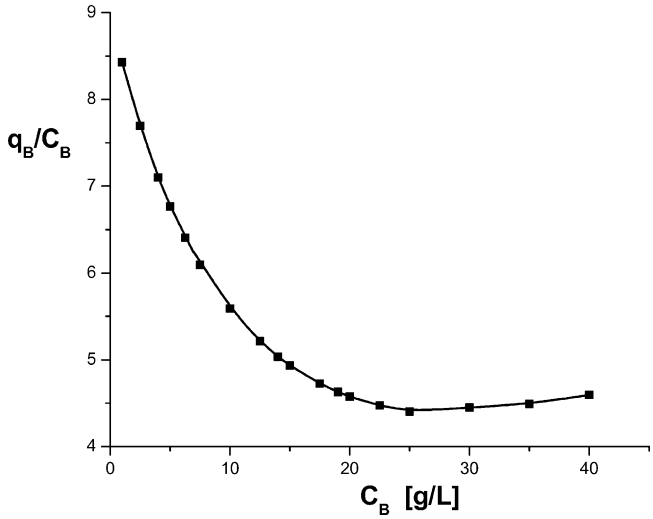

Fig. 9. Plot of the competitive isotherm chord of 4-*tert*-butylphenol calculated from the implemented kinetic competitive model. Compare with the shapes of the predicted isotherms in Figs. 6 and 8.

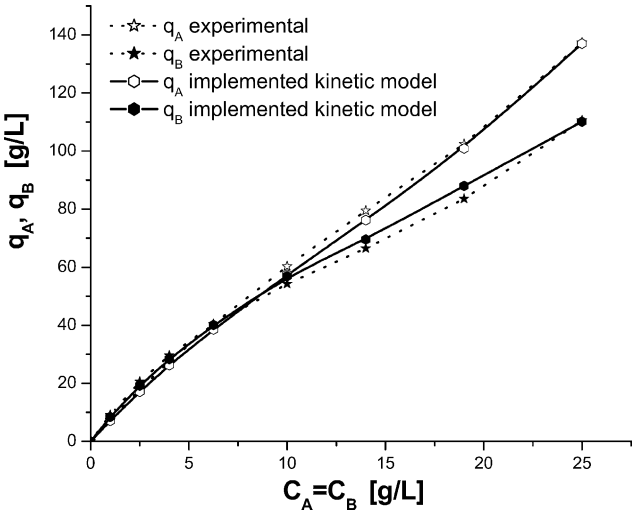

Fig. 8. Comparison between the competitive experimental isotherms of ethylbenzoate (empty stars, dotted line) and 4-*tert*-butylphenol (solid stars, dotted line) and the competitive isotherm models previously derived in Section 2.4. (connected hexagones) assuming five layers maximum in the adsorbed phase. Compare with Fig. 6 the agreement at high concentrations between experimental data and the model prediction for 4-*tert*-butylphenol.

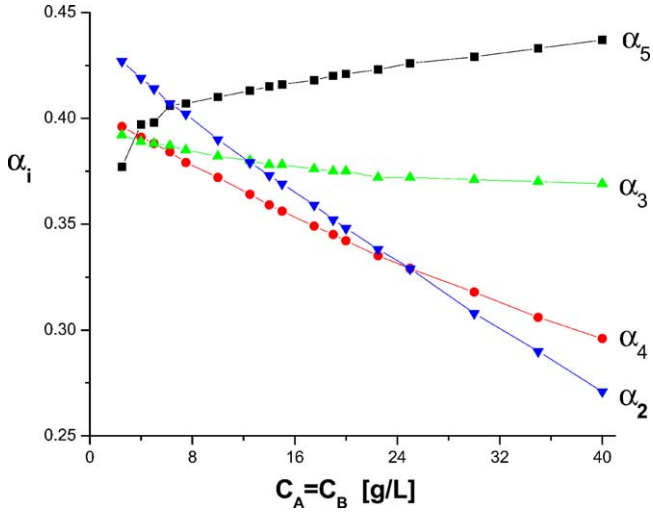

Fig. 10. Plot of the α_i values (or proportion of molecules of A adsorbed on layers made of molecules of A in the upper layers, i.e., here, layers 2, 3, 4 and 5) versus the mixture concentration in the mobile phase. The α_i are obtained after the numerical calculations have converged with 0.1%. Except for the upper layer 5, note that α_i decreases with increasing concentration of the mixture, showing that molecules of A are more often adsorbed on molecules of B than on other molecules of A.

layer ($i = 5$), α_i decreases with increasing concentration of the equimolar mixture used. In other words, the higher the concentration, the more frequently a molecule of A is adsorbed on a molecule of B in the layer directly in contact with the mobile phase. However, this physical model of the adsorbed phase, as a binary multilayer system, needs to be validated. To this purpose, we discuss, in a forthcoming paper, the calculation of overloaded band profiles using this new kinetic competitive isotherm model. This calculation is long and difficult because of the complex approach used to calculate isotherm data points and may require a completely original approach.

5. Conclusion

The new competitive isotherm model is consistent with the single-component isotherms of the two compounds studied, ethylbenzoate and 4-*tert*-butylphenol, a five layers BET and a Langmuir isotherms, respectively. This new model accounts well for the adsorption data measured by frontal analysis for equimolar mixtures of these two compounds. Two simpler models which were previously derived from a similar physical model failed to describe the experimental competitive adsorption data at high concentrations. The main discrepancy concerned the adsorption of 4-*tert*-butylphenol whose experimental isotherm is clearly S-shaped, not strictly convex upward as predicted by these earlier models. By contrast, the new kinetic model accounts well for the competitive adsorption data. The adsorption constant of 4-*tert*-butylphenol onto layers made of ethylbenzoate ($b_{B,A} = 0.0120$ l/g) is intermediate between the adsorption constant of ethylbenzoate on layers made of 4-*tert*-butylphenol ($b_{A,B} = 0.0105$ l/g) and that of ethylbenzoate on itself ($b_{A,A} = 0.0145$ l/g).

The development of this new model, despite its long derivation and its numerical definition, constitutes a progress in our understanding of the splitting of the band profiles of 4-*tert*-butylphenol when in mixtures with ethylbenzoate at high concentrations, a most unusual phenomenon. A forthcoming paper will discuss the use of this isotherm model and of the Rouchon program of calculation of overloaded band profiles in chromatography to account for this phenomenon.

Acknowledgements

This work was supported in part by grant CHE-00-70548 of the National Science Foundation and by the cooperative agreement between the University of Tennessee and the Oak Ridge National Laboratory. We thank Hans Liliedahl and Lars Torstenson (Eka Nobel, Bohus, Sweden) for the generous gift of the columns used in this work and for fruitful discussions.

Appendix A. Example of resolution: case of $N = 5$ layers → $i \in$ [1,5]

The solution of the system of Eqs. (9-iA), (9-iB) and (10) is given under the form provided by Eq. (21-iA). We write here the exact solution for γ_i, $\beta_{i,1}$ and $\beta_{i,2}$:

$$\gamma_5 = \alpha_5 + (1-\alpha_5)t_{A,B} - \frac{(1-\alpha_5)t_{A,B}^2 b_{A,B} C_A}{K_2 t_{B,A}} \quad (28\text{-}\{5,0\})$$

$$\beta_{5,1} = b_{A,A} C_A \quad (28\text{-}\{5,1\})$$

$$\beta_{5,2} = \frac{t_{A,B} b_{A,B} b_{B,A} C_A C_B}{K_2} \quad (28\text{-}\{5,2\})$$

$$\gamma_4 = \alpha_4 + (1-\alpha_4)t_{A,B} + b_{A,A} C_A - \frac{\alpha_5 \beta_{5,1}}{\gamma_5} - \frac{(1-\alpha_4)t_{A,B}^2 b_{A,B} C_A}{K_2 t_{B,A}} \quad (28\text{-}\{4,0\})$$

$$\beta_{4,1} = b_{A,A} C_A + \frac{\alpha_4 \beta_{4,2}}{\gamma_4} \quad (28\text{-}\{4,1\})$$

$$\beta_{4,2} = \frac{t_{A,B} b_{A,B} b_{B,A} C_A C_B}{K_2} \quad (28\text{-}\{4,2\})$$

$$\gamma_3 = \alpha_3 + (1-\alpha_3)t_{A,B} + b_{A,A} C_A + t_{B,A} b_{B,A} C_B \frac{K_2 - 1}{K_2} - \frac{\alpha_4 \beta_{4,1}}{\gamma_4} - \frac{(1-\alpha_3)t_{A,B}^2 b_{A,B} C_A}{K_2 t_{B,A}} - \frac{(1-\alpha_5)t_{A,B} \beta_{5,1} \beta_{4,1}}{K_2 \gamma_5 \gamma_4} - \frac{(1-\alpha_5)t_{A,B} \beta_{5,2}}{K_2 \gamma_5} \quad (28\text{-}\{3,0\})$$

$$\beta_{3,1} = b_{A,A} C_A + \frac{\alpha_4 \beta_{4,2}}{\gamma_4} + \frac{(1-\alpha_5)t_{A,B} \beta_{5,1} \beta_{4,2}}{K_2 \gamma_5 \gamma_4} \quad (28\text{-}\{3,1\})$$

$$\beta_{3,2} = \frac{t_{A,B} b_{A,B} b_{B,A} C_A C_B}{K_2} \quad (28\text{-}\{3,2\})$$

$$\gamma_2 = \alpha_2 + (1-\alpha_2)t_{A,B} + b_{A,A} C_A + t_{B,A} b_{B,A} C_B \frac{K_2 - 1}{K_2} - \frac{\alpha_3 \beta_{3,1}}{\gamma_3} - \frac{(1-\alpha_2)t_{A,B} r_{A,B} b_{A,B} C_A}{K_1} - \frac{(1-\alpha_4)t_{A,B} \beta_{4,1} \beta_{3,1}}{K_2 \gamma_4 \gamma_3} - \frac{(1-\alpha_4)t_{A,B} \beta_{4,2}}{K_2 \gamma_4} \quad (28\text{-}\{2,0\})$$

$$\beta_{2,1} = b_{A,A} C_A + \frac{\alpha_3 \beta_{3,2}}{\gamma_3} + \frac{(1-\alpha_4)t_{A,B} \beta_{4,1} \beta_{3,2}}{K_2 \gamma_4 \gamma_3} \quad (28\text{-}\{2,1\})$$

$$\beta_{2,2} = \frac{t_{A,B} b_{A,B} b_{B,S} C_A C_B}{K_1} \quad (28\text{-}\{2,2\})$$

$$\gamma_1 = 1 + b_{A,A} r_{A,A} C_A + b_{B,A} r_{B,A} C_B - \alpha_2 r_{A,A} \frac{\beta_{2,1}}{\gamma_2} - \frac{r_{B,A} b_{B,A} C_B}{K_2} - \frac{(1-\alpha_3) r_{B,A} t_{A,B} \beta_{3,1} \beta_{2,1}}{K_2 t_{B,A} \gamma_3 \gamma_2} - \frac{(1-\alpha_3) r_{B,A} t_{A,B} \beta_{3,2}}{K_2 t_{B,A} \gamma_3} \quad (28\text{-}\{1,0\})$$

$$\beta_{1,1} = b_{A,S} C_A + \alpha_2 r_{A,A} \frac{\beta_{2,2}}{\gamma_2} + \frac{(1-\alpha_3) r_{B,A} t_{A,B} \beta_{3,1} \beta_{2,2}}{K_2 t_{B,A} \gamma_3 \gamma_2} \quad (28\text{-}\{1,1\})$$

$$\beta_{1,2} = 0 \quad (28\text{-}\{1,2\})$$

In this first part of the calculation, the α_i are assumed to be all equal to the initial guess, α (Eq. (18)). A first approximation of the composition of the upper layers 1–5 is then easily achieved (i.e., all the θ fractions are known).

The surface fractions, φ, describing the composition of the different sublayers, 1–4 of the adsorbed system below each upper layer can now be obtained numerically as follows.

A.1. Upper layer, $i = 5$

First, from the equilibrium Eqs. (22-{3,5}) and (22-{1,5}), the normalization Eq. (24-{1,5}) and the model Eqs. (25-{1,5}) and (25-{2,5}), we express $\varphi_{A,B,4,5}$ as a function of $\theta_{A,B,5}$, $\theta_{A,A,5}$, $\varphi_{B,2,5}$ and $\varphi_{B,1,5}$:

$$\varphi_{A,B,4,5} = \frac{\varphi_{B,2,5}}{\varphi_{B,1,5}} \sqrt{K_S B_5 (\theta_5 - \varphi_{B,1,5})} \quad (29)$$

with

$$B_5 = \frac{\theta_{A,B,5}^2}{\theta_{A,A,5}} \quad (30)$$

Second, from the equilibrium Eq. (22-{2,5}), the normalization Eqs. (24-{2,5}) and (29), we express $\varphi_{A,A,4,5}$ as a function of B_5, $\varphi_{B,2,5}$ and $\varphi_{B,1,5}$:

$$\varphi_{A,A,4,5} = \frac{(\theta_5 - \varphi_{B,1,5} - \varphi_{B,2,5})}{\varphi_{B,1,5}^2} K_S B_5 (\theta_5 - \varphi_{B,1,5}) \quad (31)$$

Finally, from the model Eq. (25-{4,5}) and the normalization Eq. (24-{4,5}), on the one hand, and from the model Eq. (25-{3,5}) and the normalization Eq. (24-{3,5}), on the other hand, we obtain the following two equations-two unknowns system:

$$\theta_5 = \theta_{A,B,5} + \frac{\varphi_{B,2,5}}{\varphi_{B,1,5}} \sqrt{K_S B_5 (\theta_5 - \varphi_{B,1,5})} + \frac{(\theta_5 - \varphi_{B,1,5} - \varphi_{B,2,5})}{\varphi_{B,1,5}^2} K_S B_5 (\theta_5 - \varphi_{B,1,5}) \quad (32\text{-}1)$$

$$\theta_5 = \frac{\varphi_{B,2,5}}{\varphi_{B,1,5}} \sqrt{K_S B_5 (\theta_5 - \varphi_{B,1,5})} + \varphi_{B,2,5} + K_S (\theta_5 - \varphi_{B,1,5}) \frac{\varphi_{B,2,5}^2}{\varphi_{B,1,5}^2} \quad (32\text{-}2)$$

The knowledge of both $\varphi_{B,1,5}$ and $\varphi_{B,2,5}$ allows the calculation of all the other φ fractional occupancies under the upper layer, $i = 5$.

A.2. Upper layer, $i = 4$

From the equilibrium Eq. (22-{2,4}), the normalization Eq. (24-{2,4}) and the model Eq. (25-{1,4}), we express $\varphi_{A,B,3,4}$ as a function of $\theta_{A,B,4}$, $\theta_{A,A,4}$ and $\varphi_{B,1,4}$, as the solution of the second degree equation:

$$\varphi_{A,B,3,4}^2 + B_4 \varphi_{A,B,3,4} + B_4 (\varphi_{B,1,4} - \theta_4) = 0 \quad (33)$$

with

$$B_4 = \frac{\theta_{A,B,4}^2}{\theta_{A,A,4}} \quad (34)$$

Using the equilibrium Eq. (22-{1,4}), the model Eq. (25-{1,4}) and introducing the solution of Eq. (33) for $\varphi_{A,B,3,4}$, we can express $\varphi_{A,A,3,4}$ as a function of $\varphi_{B,1,4}$ only.

$$\varphi_{A,A,3,4} = K_S \left[\frac{-B_4 + \sqrt{B_4^2 + 4B_4(\theta_4 - \varphi_{B,1,4})}}{2} \right]^2 \times \frac{\theta_4 - \varphi_{B,1,4}}{\varphi_{B,1,4}^2} \quad (35)$$

Since $\varphi_{B,3,4} = \theta_{A,B,4}$ and using the normalization condition for the sublayer $k = 3$, we can solve numerically the following equation and derive $\varphi_{B,1,4}$:

$$K_S \left[\frac{-B_4 + \sqrt{B_4^2 + 4B_4(\theta_4 - \varphi_{B,1,4})}}{2} \right]^2 \frac{\theta_4 - \varphi_{B,1,4}}{\varphi_{B,1,4}^2} + \frac{-B_4 + \sqrt{B_4^2 + 4B_4(\theta_4 - \varphi_{B,1,4})}}{2} + \theta_{A,B,4} = \theta_4 \quad (36)$$

Then all the other φ values describing the adsorbed system under the upper layer, $i = 4$, are easily derived as well as the coefficient α_i from Eq. (26-{3,4}).

A.3. Upper layer, $i = 3$

Following the same procedure, from the equilibrium Eq. (22-{1,3}), we derive:

$$\varphi_{B,1,3}^2 = K_S B_3 (\theta_3 - \varphi_{B,1,3}) \quad (37)$$

With

$$B_3 = \frac{\theta_{A,B,3}^2}{\theta_{A,A,3}} \quad (38)$$

$\varphi_{B,1,3}$ is easily derived from this second degree equation.

A.4. Upper layer, $i = 2$

The solution for $\varphi_{B,1,2}$ is trivial from Eq. (24-{1,2}):

$$\varphi_{B,1,2} = \theta_{A,B,2} \quad (39)$$

References

[1] G. Guiochon, S. Golshan-Shirazi, A.M. Katti, Fundamentals of Preparative and Nonlinear Chromatography, Academic Press, Boston, MA, 1994.
[2] G. Guiochon, J. Chromatogr. A 965 (2002) 129.
[3] B. Lin, G. Guiochon, Modeling for Preparative Chromatography, Elsevier, Amsterdam, The Netherlands, 2003.
[4] A. Felinger, G. Guiochon, J. Chromatogr. A 796 (1998) 59.
[5] D.M. Ruthven, Principles of Adsorption and Adsorption Processes, Wiley, New York, NY, 1984.
[6] G. Schay, G. Szekely, Acta Chem. Hung. 5 (1954) 167.
[7] D.H. James, C.S.G. Phillips, J. Chem. Soc. (1954) 1066.
[8] E. Glueckauf, Trans. Faraday Soc. 51 (1955) 1540.
[9] E. Cremer, G.H. Huber, Angew. Chem. 73 (1691) 461.
[10] F.G. Helfferich, D.L. Peterson, J. Chem. Educ. 41 (1964) 410.
[11] H. Poppe, J. Chromatogr. A 656 (1993) 19.
[12] F. Charton, M. Bailly, G. Guiochon, J. Chromatogr. A 687 (1998) 13.
[13] J.-X. Huang, G. Guiochon, J. Coll. Interf. Sci. 128 (1989) 577.
[14] J. Jacobson, J.H. Frenz, Cs. Horváth, J. Chromatogr. 316 (1984) 53.
[15] Z. Ma, A. Katti, B. Lin, G. Guiochon, J. Phys. Chem. 94 (1990) 6911.
[16] J. Zhu, A. Katti, G. Guiochon, J. Chromatogr. 552 (1991) 71.
[17] I. Quiñones, J.C. Ford, G. Guiochon, Chem. Eng. Sci. 55 (2000) 909.
[18] F. Gritti, G. Guiochon, J. Chromatogr. A 1008 (2003) 23.
[19] F. Gritti, G. Guiochon, J. Chromatogr. A 1008 (2003) 13.
[20] J. Jacobson, J.H. Frenz, Cs. Horváth, Ind. Eng. Chem. Res. 26 (1987) 43.
[21] S. Brunauer, P.H. Emmet, E. Teller, J. Am. Chem. Soc. 60 (1938) 309.
[22] F. Gritti, W. Piatkowski, G. Guiochon, J. Chromatogr. A 978 (2002) 81.
[23] A.L. Myers, J.M. Prausnitz, AIChE J. 11 (1965) 121.
[24] C.J. Radke, J.M. Prausnitz, AIChE J. 18 (1972) 761.
[25] M. Kele, G. Guiochon, J. Chromatogr. A 855 (1999) 423.
[26] F. Gritti, G. Guiochon, J. Chromatogr. A 1003 (2003) 43.
[27] A. Felinger, F. Gritti, G. Guiochon, J. Chromatogr. A 1017 (2003) 45.